



## Partitioning of amino-acid analogues in a five-slab membrane model

Durba Sengupta<sup>a,1</sup>, Jeremy C. Smith<sup>a,b</sup>, G. Matthias Ullmann<sup>c,\*</sup>

<sup>a</sup> IWR – Computational Molecular Biophysics, University of Heidelberg, Im Neuenheimer Feld 368, 69120 Heidelberg, Germany

<sup>b</sup> UT/ORNL Center for Molecular Biophysics, Oak Ridge National Laboratory, 1 Bethel Valley Road Oak Ridge TN 37831, USA

<sup>c</sup> Structural Biology/Bioinformatics, University of Bayreuth, Universitätsstr. 30, BGI, 95447 Bayreuth, Germany

### ARTICLE INFO

#### Article history:

Received 19 October 2007

Received in revised form 15 May 2008

Accepted 17 June 2008

Available online 28 June 2008

#### Keywords:

Amino-acid positional preference

Membrane partitioning

Snorkeling

Five-slab membrane model

Poisson-Boltzmann electrostatics

### ABSTRACT

The positional preferences of the twenty amino-acid residues in a phospholipid bilayer are investigated by calculating the solvation free energy of the corresponding side chain analogues using a five-slab continuum electrostatic model. The side-chain analogues of the aromatic residues tryptophan and tyrosine are found to partition in the head-group region, due to compensation between the increase of the non-polar component of the solvation free energy at the boundary with the aqueous region and the decrease in the electrostatic component. The side chain analogue of phenylalanine differs from the other aromatic molecules by being able to partition in both the head-group region and the membrane core. This finding is consistent with experimental findings of the position of phenylalanine in membrane helices. Interestingly, the charged side-chain analogues of arginine and lysine are shown to prefer the head-group region in an orientation that allows the charged moiety to interact with the aqueous layer. The orientation adopted is similar to the “snorkelling” effect seen in lysine and arginine residues in membrane helices. In contrast, the preference of the charged side-chain analogues of histidine (protonated) and aspartate (deprotonated) for the aqueous layer is shown to be due to a steep decrease in the electrostatic component of the solvation free energy at the boundary to the aqueous region. The calculations allow an understanding of the origins of side chain positioning in membranes and are thus useful in understanding membrane–protein:lipid thermodynamics.

© 2008 Elsevier B.V. All rights reserved.

### 1. Introduction

The structure and topology of membrane proteins is determined by interactions of the membrane-bound peptides with each other, the lipid bilayer and water molecules [1,2]. Differences between protein–water and protein–lipid interactions give rise to different positional preferences of the various amino-acid residues, some preferring the aqueous phase, some the head group region and others the membrane core. Positional preferences in amino-acid distributions have been found in the analysis of experimental data on membrane proteins [3–5]. Positional preferences have also been seen in studies on a number of model synthetic peptides [6–12] and side-chain analogues [13,14]. Systematic analysis of partition profiles of amino acids (and amino acid analogues) as a function of the depth of membrane insertion has been carried out using a number of approaches, including experimental [15], bioinformatic [16] and theoretical [17–23] methods.

As expected from their physico-chemical properties, non-polar aliphatic residues, namely alanine, valine, leucine, valine and methionine, have the strongest positional preference for the membrane core. It has been seen that there is a strong correlation between the hydro-

phobicity scales and the propensity of a given residue to be present in the hydrocarbon region [3–7,24,25]. The non-polar residues that partition in the membrane core also have a high propensity to occur in the head-group region of the membrane, though the preference for the head-group region is lowered compared to the membrane core [3]. The aromatic residues tryptophan and tyrosine interact with the head-group region, often at the level of the lipid carbonyl groups, [9,13] and are often seen as flanking residues of transmembrane segment [26]. The amino-acid phenylalanine differs from the other aromatic residues and may be present both in the membrane core and the head-group region [24]. The head group region is also enriched in polar residues i.e. serine, threonine, cysteine, histidine, glycine and proline [24]. The basic amino-acid residues lysine and arginine also interact with phospholipid head-groups at the level of the phosphate group [4,11–14]. In the bilayer, these residues may “snorkel” out and reach into the lipid head-group region even when positioned in the membrane core [24,27]. In contrast, the acidic polar amino-acid residues, such as aspartate and glutamate, are rarely present within the membrane and, if present, are usually buried inside helical bundles [3,4,28].

An increasing number of theoretical studies focus on the partitioning behavior of amino-acid residues. The positional preference of indole for the head group region has been reproduced by an implicit model [29] and was shown to be due to preferable interaction of the indole  $\pi$ -electron cloud with the lipid head groups [30,31]. The

\* Corresponding author.

E-mail address: [Matthias.Ullmann@uni-bayreuth.de](mailto:Matthias.Ullmann@uni-bayreuth.de) (G.M. Ullmann).

<sup>1</sup> Current address: GBB, University of Groningen, 9747 AG Groningen, Netherlands.

partitioning behavior of all amino-acid residues has also been examined with generalized-Born models [17,22] and with molecular dynamics simulations [21,32]. Molecular dynamics simulations of model hydrophobic peptides containing polar amino-acid residues at defined positions [18,22,33] have provided partition profiles similar to the biological scale [15]. Advances in this field have led to developments of databases such as the OPM database that provides spatial arrangements of membrane proteins with respect to the hydrocarbon core of the lipid bilayer [34].

Although the above studies reproduce reasonably well the positioning of the amino-acids in membranes, the energetics and the driving forces of the partitioning behavior are less well understood. The elucidation and decomposition of the driving forces of the partitioning behavior using a theoretical model would allow a fundamental understanding of lipid–peptide interactions and provide a step in the direction of membrane protein structure prediction. In this paper, the energetics of the positional preferences of the twenty amino-acid residues in the membrane are investigated via calculation and analysis of the solvation free energy of the corresponding side-chain analogues using the Poisson–Boltzmann equation. Side-chain analogues, rather than the amino-acid residues themselves, are studied to avoid backbone effects which differ between free amino acids and those bound in secondary structural elements. A five-slab implicit membrane model that distinguishes between the membrane head-group region, membrane core and the aqueous region is used. This five-slab model has been previously used by the authors to understand the orientations [35] and macromolecular electrostatics [36] of membrane helices. The method is extended here to include a non-polar energy cost in the head-group region. Simple electrostatic models, such as the one used here, have the advantage to be tractable by a human mind, while all-atom simulations are often difficult to understand and to dissect. The experimental positional preference of all amino-acid residues is reproduced by the calculations. The partitioning of the tryptophan and tyrosine residues in the head-group region is analyzed, and the reason for the reduced affinity of phenylalanine for the head-group region is elucidated. The “snorkelling” effect of lysine is also examined and shown to be influenced by side-chain orientation. The results obtained here, allow a deeper understanding of lipid–peptide interactions.

## 2. Methods

The free energy  $\Delta G_{\text{solv}}$  for transferring the molecule from vacuum into a given position and orientation in the membrane [37] is computed and the most probable position of a membrane-bound molecule is determined by its minimum. The solvation energy is calculated as described below, using an all-atom model for the molecule embedded in a five-slab continuum dielectric membrane model.

### 2.1. The five-slab membrane model

In the model, the biological membrane is represented implicitly by five continuum dielectric slabs as shown in Fig. 1. The model is an extension of a similar model that has been used previously to understand orientations of membrane helices [35]. The unique feature of the model is the distinction between the solvent, head-group and core regions. The outermost slabs correspond to the bulk aqueous phase, and the innermost slab corresponds to the membrane core. The two slabs in between correspond to the lipid head-group regions of the membrane.

The outermost slabs of the model, i.e., those representing the aqueous phase, are assigned a relative dielectric constant of 80, corresponding to the high polarity of bulk water. The thickness of the aqueous slabs is allowed to vary with the desired system size. The innermost slab is comprised of the non-polar long-chain fatty acids with a relative dielectric constant of 2 [38,39]. A typical width of the

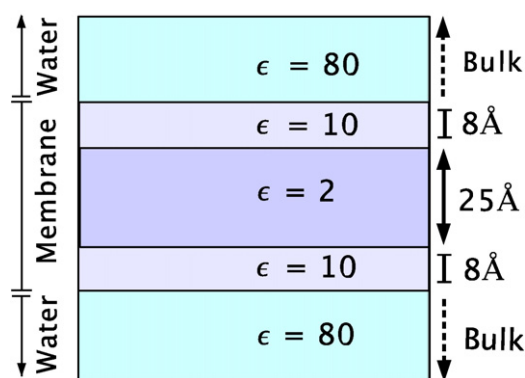


**Fig. 1.** Five-slab continuum electrostatic model of a biological membrane environment. The membrane is represented as three slabs corresponding to the two head-group regions and the core region. The head-group region is modelled as a 8 Å slab on either side of the low dielectric core region. The two outer slabs correspond to bulk water. The dielectric constants assigned to the regions are shown in the figure.

core region is 25 Å (c.f. Fig. 1). The head-group region is heterogeneous with varying fractions of phosphatidylethanolamines, phosphatidylserines, phosphatidylcholines, sphingomyelin, glycolipids and cholesterol. Estimates of the dielectric constant of the head-group region have yielded varying results depending in part on the lipid moieties present [38–43]. However, the polarity of the head-group region in phosphatidylcholine and phosphatidylserine bilayers has been found to be intermediate between that of bulk water and the bilayer core [42,43]. A value of 10 for the dielectric constant for the head-group slab has been found to accurately reproduce experimental studies of adsorption of small molecules into the head-group region [41]. In the present case, a dielectric constant of 10 was used with a slab width of 8 Å. The reasonableness of this value was tested by varying the dielectric constant between 8–18 for three test cases, namely butane, imidazolium and indole. The maximum deviation in  $\Delta G_{\text{solv}}$  with respect to the value at  $\epsilon = 10$ , was found to be less than 3%.

### 2.2. Calculation of solvation free energy

$\Delta G_{\text{solv}}$  was calculated according to the thermodynamic cycle shown in Fig. 2.  $\Delta G_{\text{solv}}$  is a sum of two contributions:

$$\Delta G_{\text{solv}} = \Delta G_{\text{elec}} + \Delta G_{\text{np}} \quad (1)$$

where  $\Delta G_{\text{elec}}$  is the electrostatic component of the solvation free energy which arises from the polarization of the environment and  $\Delta G_{\text{np}}$  is the non-polar component of the solvation free energy which arises from the cost to form a cavity in the solvent.

$\Delta G_{\text{elec}}$  is the electrostatic energy required to transfer the molecule from vacuum to a given position in the membrane. It is given by the difference of the energy required to charge the molecule in the membrane  $\Delta G_{\text{elec}}^{\text{mem}}$  and in vacuum  $\Delta G_{\text{elec}}^{\text{vac}}$ :

$$\Delta G_{\text{elec}} = \Delta G_{\text{elec}}^{\text{mem}} - \Delta G_{\text{elec}}^{\text{vac}} \quad (2)$$

$\Delta G_{\text{elec}}^{\text{mem}}$  and  $\Delta G_{\text{elec}}^{\text{vac}}$  can be calculated from:

$$\Delta G_{\text{elec}}^{\text{mem/water}} = \sum_i \frac{q_i \phi_i}{2} \quad (3)$$

$\phi_i$  can be obtained numerically by solving the linear Poisson–Boltzmann equation relating the variation in the electrostatic potential  $\phi$  to the spatially dependent dielectric permittivity  $\epsilon(r)$  and the spatial distribution of point charges  $q_i$ . The finite difference method [44] implemented in the CHARMM [45] software package (version 30b1) was used. The ionic strength was set to 0.15 M. The electrostatic potentials were calculated using the focussing technique on a grid with spacing 1.0 Å, 0.5 Å and 0.25 Å. In all calculations,

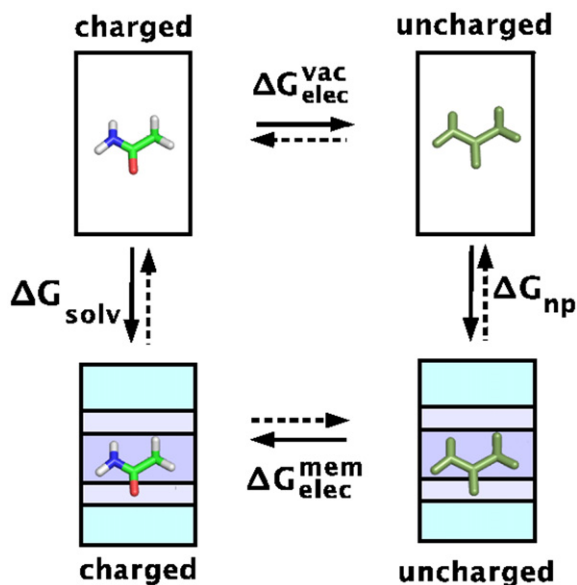


**Fig. 2.** Four-step thermodynamic cycle to calculate  $\Delta G_{\text{solv}}$  for a molecule in a membrane.  $\Delta G_{\text{elec}}^{\text{mem}}$  and  $\Delta G_{\text{elec}}^{\text{vac}}$  correspond to the energy of charging the peptide in the membrane and in vacuum, respectively. The non-polar contribution  $\Delta G_{\text{np}}$  is the cost of cavity formation in the surrounding solvent.

the distance between the grid boundaries and the molecular surface was set to at least 15 Å. The atomic radii of the atom types were taken as the calculated Born radii [46]. A cardinal *b*-spline was used for distributing charges over the grid points. The temperature was set to 300 K and no membrane potential was applied. The electrostatic potentials in the membrane environment and in vacuum ( $\epsilon=1$ ) were calculated. The corresponding solvation free energies of the system in the membrane  $\Delta G_{\text{elec}}^{\text{mem}}$  and in vacuum  $\Delta G_{\text{elec}}^{\text{vac}}$  were computed from these potentials using Eq. (3).

$\Delta G_{\text{np}}$  is the non-polar component of the solvation free energy, often referred to as the cost of cavity formation. It has been found to be linearly proportional to the solvent-accessible surface area of the molecules [47]. Here,  $\Delta G_{\text{np}}$  is calculated as the sum of two components – the non-polar free energy contribution in water  $\Delta G_{\text{np}}^{\text{aq}}$  and the non-polar free energy contribution in the head-group region  $\Delta G_{\text{np}}^{\text{hg}}$ .

The aqueous component  $\Delta G_{\text{np}}^{\text{aq}}$  is given by:

$$\Delta G_{\text{np}}^{\text{aq}} = \gamma^{\text{aq}} A^{\text{aq}} + b^{\text{aq}} \quad (4)$$

where  $A^{\text{aq}}$  is the water-accessible surface area of the molecule in the aqueous phase and  $\gamma^{\text{aq}}$  and  $b^{\text{aq}}$  are constants. The proportionality constant  $\gamma^{\text{aq}}$  is referred to as the “surface tension coefficient” and represents the contribution to the solvation free energy per unit surface area [48,49]. The constant  $b^{\text{aq}}$  is the free energy of hydration for a point solute *i.e.*, for which  $A^{\text{aq}}=0$ .

The values used are  $\gamma^{\text{aq}}=2.78 \times 10^{-2}$  kcal/mol Å<sup>2</sup> and  $b^{\text{aq}}=-1.71$  kcal/mol and were derived from the partitioning of alkanes between liquid alkane and water [48]. Thus, the non-polar interactions between the lipid and the solute molecule are considered implicitly. The values of  $\gamma^{\text{aq}}$  and  $b^{\text{aq}}$  have been used earlier for calculations on membrane proteins and compare well with experimental results [49–51].

The membrane component  $\Delta G_{\text{np}}^{\text{hg}}$  is calculated similarly:

$$\Delta G_{\text{np}}^{\text{hg}} = \gamma^{\text{hg}} A^{\text{hg}} + b^{\text{hg}} \quad (5)$$

where  $A^{\text{hg}}$  is the solvent-accessible surface area of the molecule in the head-group region and  $\gamma^{\text{hg}}$  and  $b^{\text{hg}}$  are constants.  $b^{\text{hg}}$  is set to zero, *i.e.*, the free energy of solvation for a point solute in the head-group region is zero. The value of  $\gamma^{\text{hg}}$  used is  $5.6 \times 10^{-4}$  kcal/mol Å<sup>2</sup> and is

about fifty times smaller than that of water,  $\gamma^{\text{aq}}$ , corresponding to the smaller value of the interfacial surface tension of phosphatidylcholine bilayers ( $\gamma=1.756 \times 10^{-3}$  N/m) [52] compared to water ( $\gamma=726 \times 10^{-3}$  N/m). Variation of this parameter for butane and indole between  $4.5 \times 10^{-4}$  kcal/mol Å<sup>2</sup> and  $6.5 \times 10^{-4}$  kcal/mol Å<sup>2</sup> resulted in a deviation of  $\Delta G_{\text{np}}$  by less than 0.05 kcal/mol.

The solvent-accessible surface areas,  $A^{\text{hg}}$  and  $A^{\text{aq}}$  were calculated using the Lee and Richards algorithm [53] implemented in the CHARMM software package. A probe sphere of radius 1.4 Å was used in all calculations.

### 2.3. Model construction

The side chain analogues studied here and the corresponding amino-acid residues are listed in Table 1. All-atom models of the side chain analogues were constructed from the CHARMM parameter set [45]. The parameters for ethylammonium and butylammonium were constructed from the parameters of methylammonium and lysine. The molecules were positioned along the membrane normal and  $\Delta G_{\text{solv}}$  was calculated. The depth of membrane insertion *v* was calculated as the distance of the center of mass of the molecule from the center of the membrane. The results are presented for the orientation in which the molecules are perpendicular to the membrane normal to best fit the side chain orientations in membrane peptides. Further orientations, such as snorkelling effects in lysine, are discussed where appropriate.

## 3. Results

The most favorable position for a molecule in a membrane is that with minimum solvation free energy. The solvation free energies of twenty two side-chain analogues (corresponding to the twenty amino acids) listed in Table 1 were calculated as a function of distance along the membrane normal. For the discussion of the results, the molecules are grouped together as aliphatic alkanes, aromatic non-polar, aliphatic substituted (containing N, S or O), and polar molecules. The implications for the positioning of the corresponding amino-acid residues in membrane peptides and proteins, such as anchoring residues, are also discussed.

**Table 1**

The side-chain analogues studied in this publication and their corresponding amino-acid residues

Amino-acid residue	Molecule analogue
Isoleucine	Butane
Alanine	Ethane
Valine	Propane
Leucine	Isobutene
Glycine	Glycine
Methionine	Ethylmethylsulphide
Cysteine	Methanethiol
Cysteine	Methanethiolate
Tryptophan	Indole
Tyrosine	Phenol
Phenylalanine	Benzene
Serine	Ethanol
Threonine	Propanol
Arginine	Guanidium
Arginine	Met-guanidium
Histidine (protonated)	Imidazolium ion
Histidine (deprotonated)	Imidazole
Lysine (protonated)	Ethylammonium
Lysine (protonated)	Butylammonium
Asparagine	Acetamide
Aspartic Acid (deprotonated)	Acetate ion
Aspartic Acid (protonated)	Acetic acid
Proline	Prolineamide
Proline	Acetylprolineamide

### 3.1. Why do we study side-chain analogues?

In the five-slab membrane model, the free energy minimum for ethane, the side-chain analogue of alanine, lies in the membrane core, consistent with experimental and bioinformatic studies on the partitioning of this amino-acid (Fig. 3). In contrast, the partitioning behavior of the entire amino-acid alanine with blocked, charged, or no termini is substantially different and the free energy minimum shifts to the head-group region. The difference arises mainly due to the unscreened partial charges on the backbone that increase the polarity of the system. Amino-acid residues in membrane proteins are, however, usually embedded in secondary-structural elements such as transmembrane helices and sheets. The hydrogen bonds in the secondary structural elements effectively neutralize the backbone partial charges. Interestingly, the partitioning behavior of the alanine in membrane proteins is reproduced in calculations in which the partial charges on the backbone atoms are set to zero. In fact, the partition profiles of the side-chain analogue and the amino-acid with zeroed backbone charges are similar and consistent with bioinformatic and experimental partitioning data on alanine residues in membrane proteins. These profiles point to the fact that partitioning in membrane proteins is dictated by the side-chain partitioning and the role of the backbone atoms is negligible. Therefore, we focus in the rest of the study on side-chain analogues.

### 3.2. Like favors like: aliphatic residues partition in the membrane core

The most favorable position for the aliphatic, non-polar side-chain analogues is in the membrane region as expected from their physico-chemical properties.  $\Delta G_{\text{solv}}$  vs. the distance  $v$  from the center of the membrane is plotted in Fig. 4 for butane (carbon chain parallel to the membrane plane), the side chain analogue of isoleucine. The value of  $\Delta G_{\text{solv}}$  is small in the membrane and increases sharply when the molecule enters the aqueous region, due to the increase of  $\Delta G_{\text{np}}$ . The decrease of  $\Delta G_{\text{elec}}$  when the molecule moves from the core to the head-group region is balanced by an increase of  $\Delta G_{\text{np}}$  resulting in a marginal increase in free energy on entering the membrane head-group region. Though the propensities of the non-polar residues to be present in the membrane core are high, their decreased preference for the head-group region is not seen in this model. The other aliphatic, non-polar side-chain analogues such as ethane, propane and isobutane show similar  $\Delta G_{\text{solv}}$  profiles and also partition in the mem-

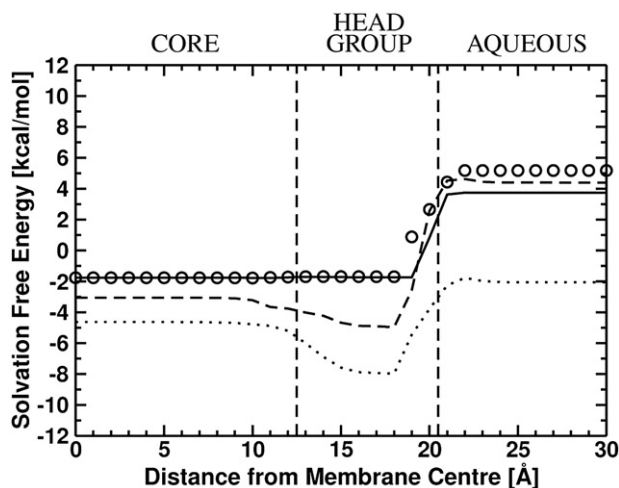


Fig. 3.  $\Delta G_{\text{solv}}$  as a function of the distance  $v$  from the center of the membrane for alanine with blocked termini (---), no termini (···) and zero back-bone charges (o o o). The profile for the side-chain analogue, ethane is also shown (—). The boundaries of the membrane core, membrane head-group and aqueous regions are marked by the dashed lines.

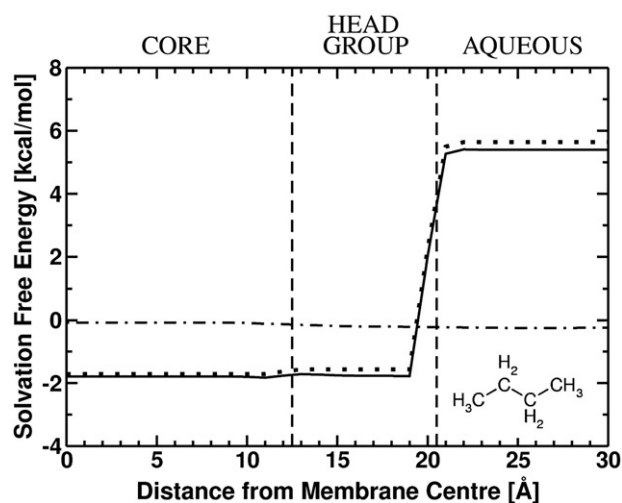


Fig. 4.  $\Delta G_{\text{solv}}$  (—) as a function of the distance  $v$  from the center of the membrane for butane (isoleucine analogue). The electrostatic component,  $\Delta G_{\text{elec}}$  (---) and the non-polar component,  $\Delta G_{\text{np}}$  (···) are also shown. The minimum value of  $\Delta G_{\text{solv}}$  is in the membrane region. The boundaries of the membrane core, membrane head-group and aqueous regions are marked by the dashed lines.

brane. This corresponds to the positioning of the residues alanine, valine and leucine in the membrane.

### 3.3. Why are membrane interfaces enriched in aromatic residues?

The side-chain analogues of the aromatic amino acid residues tryptophan, tyrosine and phenylalanine studied here are indole, phenol and benzene, respectively. Indole was placed with the ring plane parallel to the membrane normal, corresponding to its preferred orientation [14]. A diagram for  $\Delta G_{\text{solv}}$  vs. the distance  $v$  from the center of the membrane for indole is shown in Fig. 5A.  $\Delta G_{\text{solv}}$  has a distinct minimum in the head-group region and the energy difference between the head-group region and the membrane core is about 6 kcal/mol. The energy minimum in the head-group region is caused by the interplay between  $\Delta G_{\text{elec}}$  and  $\Delta G_{\text{np}}$ .  $\Delta G_{\text{elec}}$  favors polar environments while  $\Delta G_{\text{np}}$  opposes entering the aqueous layer. The strong decrease of  $\Delta G_{\text{elec}}$  on moving from the membrane center to the head-group region is not cancelled by the increase in  $\Delta G_{\text{np}}$ , which becomes significant only in the aqueous phase. The present result of indole partitioning in the head-group region agrees with NMR measurements also showing that indole partitions into the head-group region of lipid bilayers [13,14]. However, since the lipid molecules are not represented at atomic detail in the model, the specific interactions of indole with the choline moiety cannot be reproduced and the resulting bimodal distribution of indole in the head-group seen in the NMR study, is not reproduced.

$\Delta G_{\text{solv}}$  vs. the distance,  $v$  from the center of the membrane for phenol (parallel to membrane normal) is depicted in Fig. 5B. This plot shows a profile similar to that of indole with a distinct energy minimum in the head-group region. The energy profile for the orientation where the aromatic ring is in the plane of the membrane is similar. The minimum for phenol is deeper than that of indole due to its greater polarity. Thus, both tyrosine and tryptophan residues occupy preferentially the head group region.

### 3.4. How does phenylalanine differ from the other aromatic residues?

Benzene exhibits a small decrease (about 3 kcal/mol) in energy on entering the head-group region from the membrane core (Fig. 5C). The decreased polarity of benzene compared to phenol and indole accounts for the shallower energy minimum in the head-group region. Due to the small energy difference between the membrane

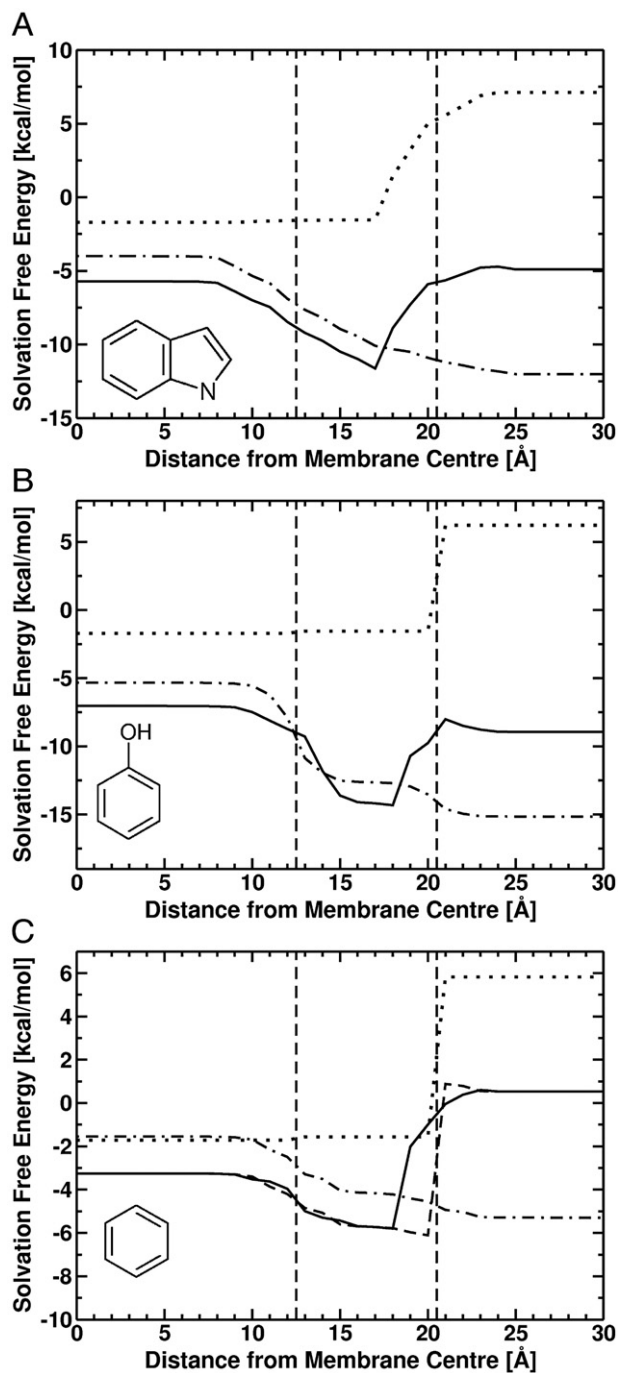


**Fig. 5.** (A)  $\Delta G_{\text{solv}}$  (—) as a function of the distance  $v$  from the center of the membrane for indole (tryptophan analogue). The electrostatic component  $\Delta G_{\text{elec}}$  (---) and the non-polar component  $\Delta G_{\text{np}}$  (···) are also shown. The minimum value of  $\Delta G_{\text{solv}}$  is in the head-group region as a result of compensation between  $\Delta G_{\text{elec}}$  and  $\Delta G_{\text{np}}$ . The membrane core, membrane head-group and aqueous regions are marked. (B)  $\Delta G_{\text{solv}}$  as a function of the distance  $v$  from the center of the membrane for phenol (tyrosine analogue). The electrostatic component  $\Delta G_{\text{elec}}$  (---) and the non-polar component  $\Delta G_{\text{np}}$  (···) are also shown. (C)  $\Delta G_{\text{solv}}$  as a function of  $v$  for benzene (phenylalanine analogue) in the membrane for two orientations: aromatic ring parallel to membrane normal (---) and in membrane plane (—). The electrostatic component  $\Delta G_{\text{elec}}$  (---) and the non-polar component  $\Delta G_{\text{np}}$  (···) are also shown.

core and head-group region, phenylalanine residues may occur in both regions.  $\Delta G_{\text{solv}}$  of two orientations of benzene are plotted in Fig. 5C: the ring plane parallel (dashed line) and perpendicular (bold line) to the membrane plane. When placed with the aromatic ring perpendicular to the membrane plane, the energy cost in the region of

the head-group region close to the aqueous phase increases, since part of the molecule enters the aqueous region. Furthermore, in contrast to phenol and indole, the solvation free energy of benzene in the aqueous phase is higher than in the membrane core. The decreased polarity of benzene compared to indole and phenol leads to a small negative value of  $\Delta G_{\text{elec}}$  that cannot compensate the  $\Delta G_{\text{np}}$  in the aqueous phase leading to a  $\Delta G_{\text{solv}}$  that is higher in the aqueous medium than in the membrane core.

### 3.5. Glycine and proline partition in the head-group region

Acetyl-prolineamide was chosen as the side-chain analogue of proline. The glycine molecule is calculated *per se*. These two molecules differ from the other studied molecules since both the backbone carbonyl and amide groups are present. The energy minimum of these two molecules is in the head-group region (Fig. 6 and Supplementary Fig. 1). Prolineamide, another side-chain analogue of proline, does not contain the acetyl group on the ring nitrogen. However, the energy profile for this molecule is similar to acetyl-prolineamide and the energy minimum lies in the head-group region. Setting the back-bone charges to zero changes the depth of the minimum but not its position (Fig. 6 and Supplementary Fig. 1).

### 3.6. Sulphur-containing residues show varied partitioning behavior

The sulphur containing residues methionine and cysteine are modelled by ethylmethylsulphide and methanethiol, respectively. In addition, the deprotonated methanethiolate, which represents cysteine in a basic environment, is also examined. The free energies of ethylmethylsulphide (carbon chain lying in the membrane plane) in the membrane core and the head-group are the same (Fig. 7). The calculated energy profile reproduces the preference of methionine for the membrane region calculated in other studies [3,24]. The gain in  $\Delta G_{\text{elec}}$  only marginally compensates the unfavorable  $\Delta G_{\text{np}}$  as the molecule traverses from the membrane core to a more polar region, thereby allowing partitioning in both the membrane core and head-group region at room temperature. Methanethiol (carbon-sulphur bond is in the membrane plane) shows an energy profile with a minimum in the head-group region (Supplementary Fig. 2A). Thus, cysteine residues have a preference for the head-group region. Upon deprotonation, the energy profile of the methanethiolate ion changes and the energy minimum shifts to the aqueous layer (Supplementary Fig. 2B).

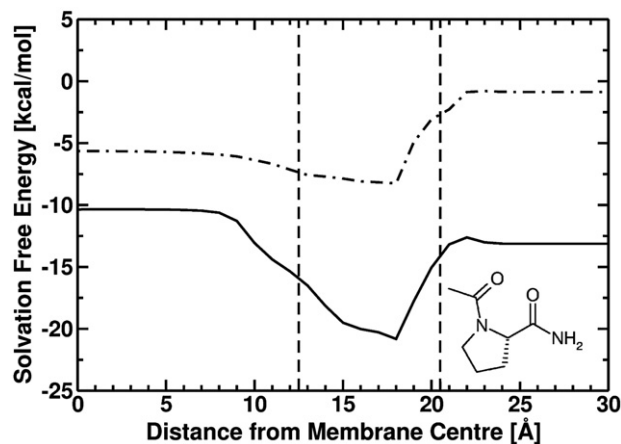


**Fig. 6.**  $\Delta G_{\text{solv}}$  as a function of the distance  $v$  from the center of the membrane for acetyl prolineamide (praline analogue) with backbone partial charges (—) and with backbone partial charges set to zero (---). The minimum value of  $\Delta G_{\text{solv}}$  is in the head group region.

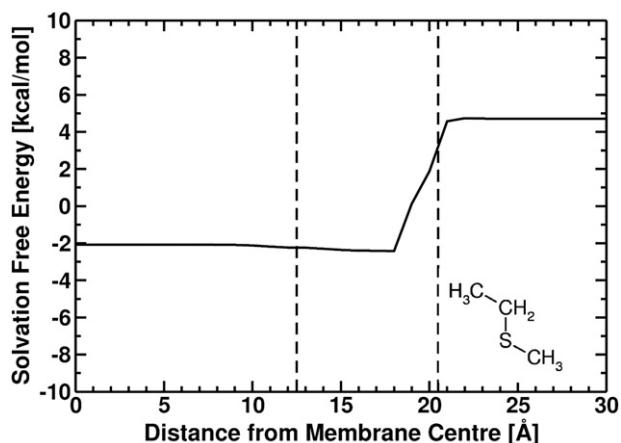


**Fig. 7.**  $\Delta G_{\text{solv}}$  as a function of the distance  $v$  from the center of the membrane for ethylmethylsulfide (methionine analogue). The energy in the membrane core and head-group region is comparable. The minimum value of  $\Delta G_{\text{solv}}$  is in the membrane. The boundaries of the membrane core, membrane head-group and aqueous regions are marked.

### 3.7. Hydroxyl-containing residues partition in the head-group region

The two alcohols studied, ethanol and propanol, are the side-chain analogues of serine and threonine, respectively. Two orientations are examined for these molecules: the hydroxyl group parallel and perpendicular to the membrane normal. The energy profile for ethanol (hydroxyl group perpendicular to membrane normal) shows an energy minimum in the head-group region (Supplementary Figure 3A). The energy minimum for ethanol in the other orientation (hydroxyl group parallel to membrane normal) also lies in the head-group region. Propanol also has an energy minimum in the head-group region (Supplementary Figure 3B) in the orientation in which the hydroxyl group is parallel to membrane normal. In this orientation, propanol exhibits an additional dip in the energy profile when the molecule is at the interface between the head-group region and the aqueous layer due to the favorable interactions of the carbonyl chain with the membrane and the hydroxyl group with the aqueous layer. The energy minimum for ethanol in the other orientation (hydroxyl group perpendicular to membrane normal) also lies in the head-group region with no additional stabilization.

### 3.8. Histidine partitioning is protonation state dependent

**Fig. 8A** shows  $\Delta G_{\text{solv}}$  vs. the distance  $v$  from the center of the membrane for the neutral imidazole molecule. The energy minimum lies in the head-group region and arises from the interplay between  $\Delta G_{\text{elec}}$  and  $\Delta G_{\text{np}}$ , similar to the case of the indole molecule above. In contrast, the protonated molecule (imidazolium) prefers the aqueous region (**Fig. 8B**). The reason for this preference is that  $\Delta G_{\text{elec}}$  decreases very rapidly when a charged molecule enters the aqueous phase, and this decrease cannot be compensated by  $\Delta G_{\text{np}}$ .

### 3.9. Positively-charged lysine can be favored in the membrane core

The role of lysine in positioning membrane helices has been extensively discussed [54,55]. Here, we study two side-chain analogues – ethylammonium and butylammonium. **Fig. 9A** shows the  $\Delta G_{\text{solv}}$  vs. the distance  $v$  from the center of the membrane for three orientations of the molecule with the amine group in the plane of the membrane (bold), tilted at  $45^\circ$  (dashed) and placed along the membrane normal (broken line). When the amine group lies in the membrane plane the energy minimum is in the aqueous layer. Tilting of the charged amine group decreases the energy in the head-group region, and when the amine group points along the membrane

normal, the head-group region is stabilized further. In the membrane normal orientation, the energy in the membrane core is lowered considerably due to reaction field stabilization of the charged amine group. Butylammonium has a longer carbon chain and shows similar energy profiles (**Fig. 9B**): the aqueous layer is preferred for the orientation in which the amide group lies in the membrane plane, tilting the amide group towards the interface stabilizes the molecule in the head-group region and aligning the amide group along the membrane normal towards the outside considerably increases the preference for the head-group region. Further, the positions inside the membrane core in which the butylammonium molecule “snorkels” into the head-group region are also stabilized. Thus, the longer carbon chain of butylammonium promotes “snorkelling” of the molecule. However, at the interface of the membrane core and head-group region, only one state is energetically favorable imposing an entropic penalty. Therefore, we suggest that lysine may partition between aqueous and head-group region depending on the orientation of the  $C_\alpha$ - $C_\beta$  bond [24,27].

### 3.10. The additional methyl group allows arginine to snorkel

Two side-chain analogues are studied for arginine: guanidinium (without the  $C_\beta$  of the amino-acid residue) and methylguanidinium. The two molecules differ in the presence or absence of a methyl group

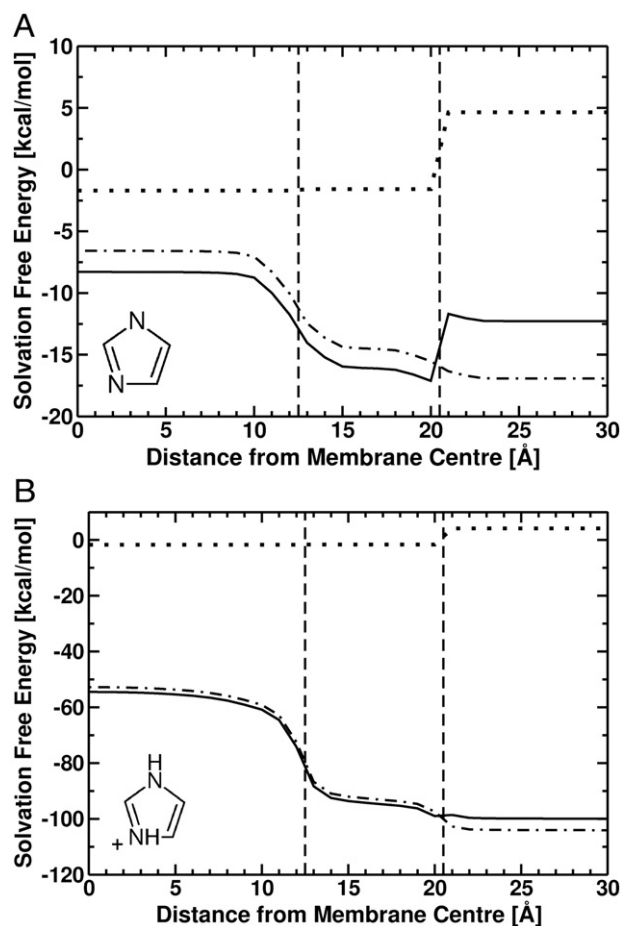


**Fig. 8.** (A)  $\Delta G_{\text{solv}}$  (—) as a function of the distance  $v$  from the center of the membrane for imidazole (analogue of deprotonated histidine). The electrostatic component  $\Delta G_{\text{elec}}$  (---) and the non-polar component  $\Delta G_{\text{np}}$  (···) are also shown. The minimum value of  $\Delta G_{\text{solv}}$  is in the head-group region. (B)  $\Delta G_{\text{solv}}$  (—) as a function of the distance  $v$  from the center of the membrane for imidazolium ion (analogue of protonated histidine). The electrostatic component  $\Delta G_{\text{elec}}$  (---) and the non-polar component  $\Delta G_{\text{np}}$  (···) are also shown. The minimum value of  $\Delta G_{\text{solv}}$  is in the aqueous region. The membrane core, membrane head-group and aqueous regions are marked.

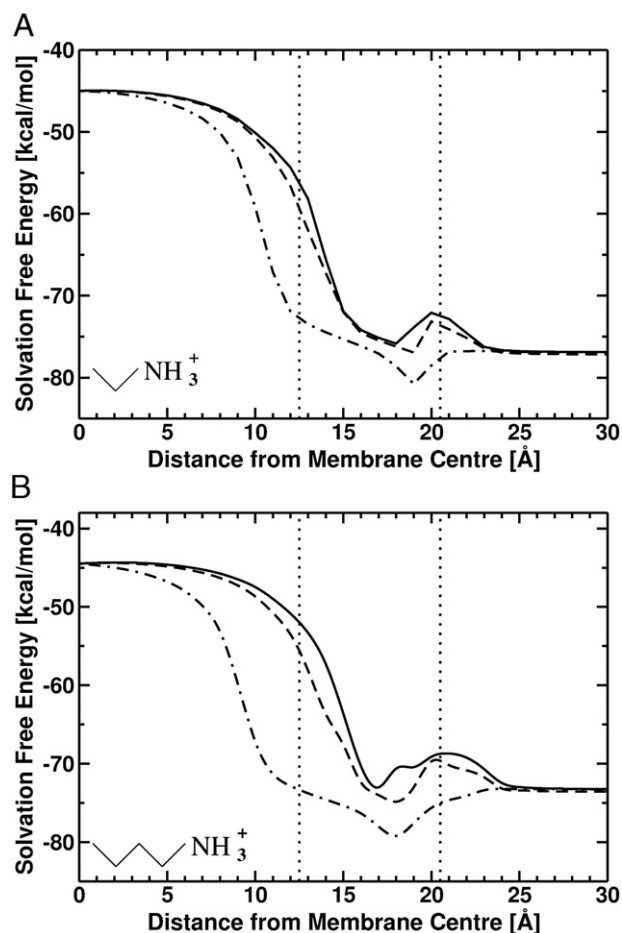


**Fig. 9.** (A)  $\Delta G_{\text{solv}}$  as a function of the distance  $v$  from the center of the membrane for ethylammonium (short lysine analogue). The energies of three orientations of the molecule are shown: the amine group in the plane of the membrane (—), the amine group tilted 45° (---) and the amine group placed along the membrane normal (-·-·). (B)  $\Delta G_{\text{solv}}$  as a function of the distance  $v$  from the center of the membrane for butylammonium (lysine analogue). The energies of three orientations of the molecule are shown: the amine group in the plane of the membrane (—), the amine group tilted 45° (---) and the amine group placed along the membrane normal (-·-·). The membrane core, membrane head-group and aqueous regions are marked.

attached to one of the nitrogen atoms. Fig. 10A shows  $\Delta G_{\text{solv}}$  vs. the distance  $v$  from the center of the membrane for guanidinium when placed in the membrane plane. The energy minimum is in the aqueous region. Interestingly, on the addition of the methyl group the energy minimum shifts to the head-group region (Fig. 10B). This shift is caused by the increase in the solvent-accessible surface area due to the additional methyl group and thus a corresponding increase in  $\Delta G_{\text{np}}$  and  $\Delta G_{\text{solv}}$  in the aqueous layer. In transmembrane segments, arginine shows a similar behavior and prefers the head-group region [4,24].

### 3.11. Negatively-charged amino-acid residues prefer the aqueous phase

Acetamide, the side-chain analogue of asparagine, partitions in the head-group region (Supplementary Fig. 4). The uncharged acetic acid (protonated) also partitions in the head-group region (Fig. 11A). Upon deprotonation, the free energy minimum of the acetate ion (side chain analogue of aspartic acid) shifts to the aqueous layer (Fig. 11B).

## 4. Discussion

### 4.1. Comparison to solvation and transfer free energies

$\Delta G_{\text{solv}}$  calculated here for the aqueous phase and membrane core, agrees well with experimental [56] and theoretical [57] estimates of

the solvation free energies of side-chain analogues in water and organic solvents, respectively. The measured cyclohexane–water transfer free energy [58] also shows a good correlation (correlation coefficient of 0.8) to the transfer free energy between membrane core and water calculated using the five-slab model (see the correlation plot in Supplementary Fig. 5A).

At the membrane interface, the energetics of amino-acid residues has been compared to an octanol environment [25,59]. The trend of the transfer free energies from water to octanol and the difference in energy between water and the head-group region match well. The White–Wimley membrane interface scale [25], which is similar to the octanol scale, also shows a good correlation with our results (Supplementary Fig. 5B).

A biological scale [15] derived from translocon-aided membrane insertion studies gives an estimate of the energetics of positioning amino-acid residues in the center of a transmembrane helix. In the study, the degree of membrane insertion of designed polypeptides is quantified and related to an apparent free energy of insertion of the amino-acid residue studied. When normalized to the insertion energy of alanine, the biological scale shows a correlation of 0.8 with the calculated transfer free energy between membrane core and water (Supplementary Fig. 5C). However, the slope of the un-normalized curve is quite low. One reason for the low slope is the systematically high deviation of the energies of the charged residues in the implicit model since we cannot consider the protonation/deprotonation cycle

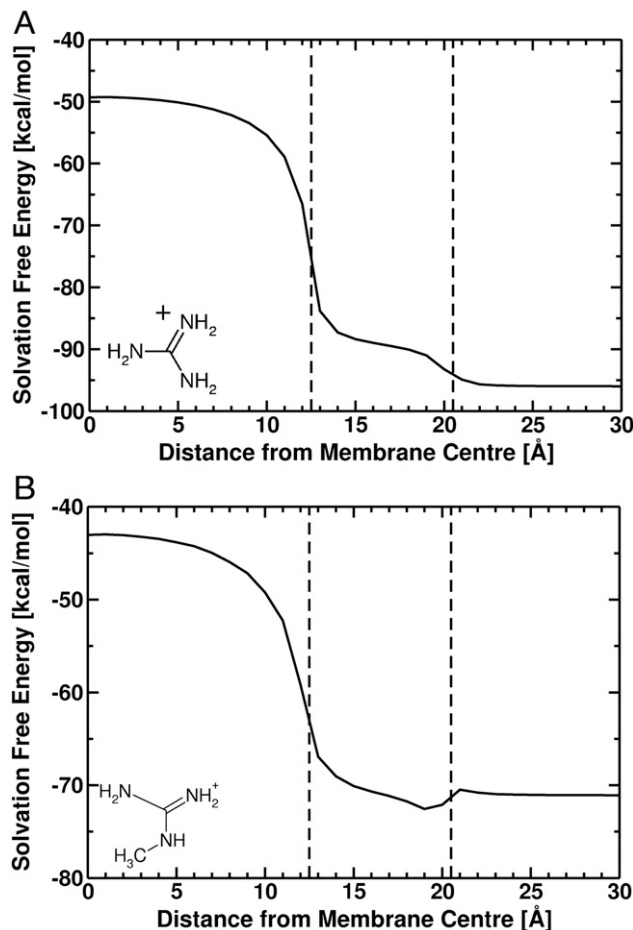


**Fig. 10.** (A)  $\Delta G_{\text{solv}}$  as a function of the distance the distance  $v$  from the center of the membrane for guanidinium (arginine analogue). The minimum value of  $\Delta G_{\text{solv}}$  is in water. (B)  $\Delta G_{\text{solv}}$  as a function of the distance  $v$  from the center of the membrane for methyl-guanidinium (arginine) when placed in the membrane plane. The energy minimum shifts to the head-group region.

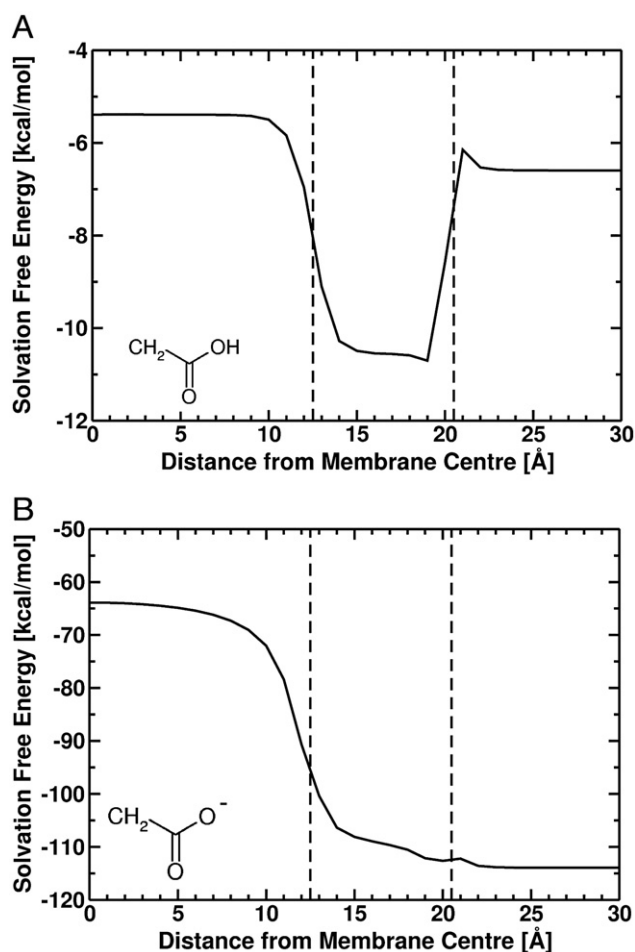


**Fig. 11.** (A)  $\Delta G_{\text{solv}}$  as a function of the distance  $v$  from the center of the membrane for acetic acid (analogue of deprotonated aspartic acid). The minimum value of  $\Delta G_{\text{solv}}$  is in the head-group region. The boundaries of the membrane core, membrane head-group and aqueous regions are marked by the dashed lines. (B)  $\Delta G_{\text{solv}}$  as a function of the distance  $v$  from the center of the membrane for acetate ion (analogue of protonated aspartic acid). The minimum value of  $\Delta G_{\text{solv}}$  is in the aqueous layer.

but consider the protonated/deprotonated species individually. Furthermore, in the biological scale, membrane insertion is also dependent on factors such as aggregation both within and outside the membrane, variable depths of insertion and tilting of the transmembrane domains, that may increase the entropy of the system but might not be relevant in the partitioning of side-chains in membrane proteins. Due to the differences in the two systems and different factors that dictate partitioning behavior, a slope of less than one is not surprising, although there is a high correlation.

#### 4.2. Comparison with partition profiles

Positional effects were seen in the biological scale on placing the residues further outwards in the helix that match the present results. A quantitative analysis is more challenging since the peptides studied simultaneously place two amino-acid residues symmetrically away from the center, corresponding to partitioning in both leaflets of the bilayer. Also, the maximum residue separation analyzed is 17 amino-acid residues, corresponding to the membrane core-head-group region interface (considering ideal helices), thus representing only a part of the partition profile.

Profiles calculated by statistical analysis of crystallographic data approaches such as analyzing the occurrence of a residue at a given location in a helix [16], also show similar patterns to those calculated here. A comparison between the calculations presented and

positions most-favored in the PDB is given in Table 2. In almost all cases, the position calculated here corresponds to the position seen in structural data. The favored position of the aliphatic residues is the membrane core in both studies, though the preference for the head-group region is increased in our study compared to the PDB distribution. The aromatic residues all partition in the head-group region in our calculations. Phenylalanine also has a high probability to be in the membrane core in our model, consistent with PDB distributions. The substituted residues such as serine, threonine and cysteine partition in the head-group region in the five-slab model though they were considered to be scattered throughout in the membrane in the bioinformatics study. However, investigation of the actual data suggests that serine and threonine indeed have a higher propensity in the head-group region. In membrane proteins, proline is seen to be mostly present outside the membrane although here the head-group region is calculated to be energetically favored. The role of proline as a “helix breaker” could be responsible for its less frequent occurrence within transmembrane helices than predicted from the present solvation free energy model. Surprisingly, the most-frequent position of lysine in membrane proteins is outside the membrane though its role as a helix anchor in the head-group region is well documented [4,11,12,24]. Our model identifies both the solvent-exposed and head-group positional preferences and elucidates how different orientations of lysine are stabilized in different environments.

The profiles calculated by a related five-slab generalized Born model match the current study closely [17]. However, a radius correction was needed in Ref [17] to match the energetics of the smaller molecules that do not pack well in the membrane. No such correction was required in the present study. The main difference with the generalized Born models is in the partitioning of the charged residues arginine and lysine. In contrast to experimental studies [4,11,12,24] and our calculated partition profiles, the stabilization in the head-group region seen in the generalized Born studies was negligibly small.

It is possible that a simpler model, such as generalized Born, cannot reproduce the fine balance between the electrostatic and non-polar energies that allows arginine and lysine to snorkel. The

**Table 2**

Comparison of the most-favored positions of side-chain residues in the membrane by the five-slab model, atomistic simulations [21] and bio-informatic studies [16]

Residue	Most favoured position		
	5-slab model	Atomistic	PDB
Isoleucine	Core	Core	Core
Alanine	Core	Core	Core
Valine	Core	Core	Core
Leucine	Core	Core	Core
Glycine	HG		Scattered
Methionine	HG	HG	HG
Cysteine (prot)	HG	HG	Scattered
Cysteine (deprot)	HG		
Tryptophan	HG	HG	HG
Tyrosine	HG	HG	HG
Phenylalanine	HG	HG	Core
Serine	HG	HG	HG*
Threonine	HG	HG	HG*
Arginine	HG	HG	HG
Histidine (prot)	AQ		AQ
Histidine (deprot)	HG		
Lysine (prot, 0°)	AQ		AQ
Lysine (prot, 90°)	HG	HG	
Asparagine	HG	HG	HG
Aspartic acid (deprot)	AQ		AQ
Aspartic acid (prot)	HG	AQ	
Proline	HG		AQ

AQ corresponds to positions in the aqueous phase and HG to the head-group region. The values of the residues marked \* are taken from the raw data since they were fitted as scattered in the study.



solvent to membrane center transfer free energies calculated by a related generalized born model [22] also match our results.

Efforts are being made to calculate the partition profiles of amino-acid residues in an atomistic membrane model [18,19,21]. Permeation of small organic molecules such as benzene, acetic acid, acetamide and methanol through the membrane has been calculated by molecular dynamics simulations with an explicit DPPC membrane [19]. The energy profiles of the molecules have generally similar shapes and preferred positions as in the current study.

The partition profile of arginine has been recently examined by calculating the free energy profile for a protonated arginine side-chain residue situated at different positions along a transmembrane helix [18]. A difference of 17 kcal/mol was calculated between the aqueous phase and the membrane core, compared to about 22 kcal/mol in the present study. These values are similar, although the calculation in Ref. [18] includes the transmembrane helix. Further, membrane defects and inclusion of water molecules around arginine, neither of which are explicitly included in a five-slab model (but see below), were shown to stabilize the arginine at positions within the membrane core.

A recent umbrella sampling study of amino acids also calculated partitioning of amino-acid analogues in a dioleoylphosphatidylcholine (DOPC) membrane [21]. The calculated energy costs are again of the same order of magnitude to those calculated here and the minimum-energy positions coincide for most residues (Table 2). Large water defects are seen for polar residues such as arginine and the authors remark that due to this, membranes should not be viewed as static low dielectric slabs. However, water incursions within the head-group region can be seen as part of the mechanisms increasing the head group dielectric constant relative to the membrane interior. Further, considering the membrane as static slabs of variable dielectric, as in the current study, does seem to enable the partitioning behavior of side chains in membranes to be accurately reproduced.

#### 4.3. Insights into partitioning of side-chains in membrane proteins

The simplicity of the five-slab membrane model allows the understanding of the key energetics that dictate partitioning behavior of amino-acid residues in membrane proteins. Comparison of the different energy terms gives a direct understanding of the costs and penalties at different positions in the membrane for a variety of side chain analogues. The partitioning behavior of the amino-acids can be understood in terms of a trade-off between  $\Delta G_{\text{elec}}$  and  $\Delta G_{\text{np}}$ . Partitioning of the aliphatic hydrophobic and the small, charged residues in the membrane core and aqueous regions, respectively, is due to a comparatively unfavorable  $\Delta G_{\text{np}}$  in the aqueous region for the aliphatic residues and highly favorable  $\Delta G_{\text{elec}}$  for the small, charged residues. For the aliphatic substituted residues (containing N, S or O), the trade-off between  $\Delta G_{\text{elec}}$  and  $\Delta G_{\text{np}}$  imposes the head-group region as being most favorable. For less polar residues, however, such as methionine, only marginal compensation occurs, leading to both the membrane core and the head-group region being accessible. The reaction field of the aqueous region also contributes to the  $\Delta G_{\text{elec}}$  and  $\Delta G_{\text{np}}$  balance, allowing the partitioning of the bulky, charged residues in the head-group region.

Comparisons between residues can also help understand differences of partitioning behavior of related molecules. Partitioning behavior of tryptophan and tyrosine is very easily seen to be due to a trade-off between the electrostatic and non-polar effects. Comparison with phenylalanine shows that the electrostatic gain in the polar head-group and aqueous region is much less, thereby leading to accessibility of even the membrane core region. Comparison of related side-chain analogues, such as guanidinium and methyl guanidinium, highlights how the addition of a single methyl group can increase the non-polar contribution and allow even charged arginine residues to partition in the head-group region. Similarly, it

is easily seen that even shorter lysine analogues, such as ethylammonium can partition in the head-group region. However, to lower the energy at the interface of the membrane core and head-group region, the additional alkyl group are necessary.

The protonation state of amino-acid residues in membrane proteins has been recently discussed [60,61]. The comprehensive study presented here also points to the feasibility of using such models for studies such as pKa calculations for amino-acid residues in membrane proteins. The model would also allow a fast screening method for calculating drug partitioning behavior in membranes and for scoring membrane protein associations.

## 5. Conclusions

The present continuum electrostatic approach uses a five-slab membrane model to determine the partitioning of various side-chain analogues in biological membranes. The solvation free energies of twenty-two side chain analogues have been calculated and shown to reproduce well the experimentally-determined positioning of the corresponding amino-acid side chains in membranes. The most favored position of the side-chain analogues in the membrane is found to coincide with the position of highest occurrence of the corresponding amino-acid residue in membrane proteins.

The results presented here help understand the energetics of side chain positioning in membrane proteins. The preference of hydrophobic residues for the membrane core is shown to arise from the higher non-polar cost on entering a more polar region compared to the electrostatic gain. This effect determines the positioning of alanine, leucine, isoleucine and valine in the membrane core. The inclusion of a small non-polar cost in the head-group region results in an increase in  $\Delta G_{\text{solv}}$  in the head-group region relative to the membrane core.

The side-chain analogues of tryptophan and tyrosine prefer the head-group region. In contrast, the preference of the side-chain analogue of phenylalanine for the head-group region is substantially reduced relative to the membrane core. The energy minima for the residues glycine and proline are also shown to lie in the head-group region. The side-chain analogue of methionine favors the membrane core, whereas that of cysteine prefers the head-group region, due to the higher polarity of the -SH group of cysteine compared to the -SMe in methionine. The side-chain analogues of serine and threonine are also found to partition into the head-group region. These results are consistent with the statistical distribution of amino acid residues in membrane proteins.

Small charged residues, such as the imidazolium and acetate ions (side-chain analogues of histidine and aspartic acid respectively), favor the aqueous layer. The acetate ion is seen to partition in the aqueous phase whereas acetamide (side-chain analogue of asparagine) partitions in the head-group region. Larger molecules, such as methyl-guanidinium, are also seen to partition in the head-group region whereas guanidinium prefers the aqueous layer. Thus, net charge is insufficient to guarantee partitioning into the aqueous phase. Butylammonium is seen to favor the head-group region if placed along the membrane normal. In this orientation, the charged moiety is stabilized by the reaction field whereas the methyl groups may interact with a region of lower polarity. This behavior corresponds to the snorkelling seen in lysine residues.

The present work demonstrates that a relatively simple electrostatic model together with a surface term is able to reproduce and facilitates the understanding of the experimentally-observed distribution of amino-acids in the membrane. The balance between the electrostatic term and the surface term is essential for obtaining the correct distributions. An understanding of the physical basis for the behavior of amino-acid residues in biological membranes is a prerequisite for successfully predicting membrane protein structures and membrane protein interactions and future developments

of models such as that introduced here will be directed towards these goals.

## Appendix A. Supplementary data

Supplementary data associated with this article can be found, in the online version, at doi:10.1016/j.bbamem.2008.06.014.

## References

- [1] S.H. White, W.C. Wimley, Membrane protein folding and stability: physical principles, *Annu. Rev. Biophys. Biomol. Struct.* 28 (1999) 319–336.
- [2] V. Helms, Attraction within the membrane: Forces behind transmembrane protein folding and supramolecular complex assembly, *EMBO reports* 3 (2002) 1133–1138.
- [3] L. Adamian, V. Nanda, W.F. DeGrado, J. Liang, Empirical lipid propensities of amino acid residues in multispan alpha helical membrane proteins, *Proteins* 59 (2005) 496–509.
- [4] T.A. Eyre, L. Partridge, J.M. Thornton, Computational analysis of  $\alpha$ -helical membrane protein structure: implications for the prediction of 3d structural models, *Prot. Eng. Des. Sel.* 17 (2004) 613–624.
- [5] M.B. Ulmschneider, M.S.P. Sansom, Amino acid distributions in integral membrane protein structures, *Biochim. Biophys. Acta* 1512 (2001) 1–14.
- [6] B. Bechinger, Membrane insertion and orientation of polyaniline peptides: a  $^{15}\text{N}$  solid state NMR spectroscopy investigation, *Biophys. J.* 81 (2001) 2251–2256.
- [7] P. Braun, G.H. Heijne, The aromatic residues Trp and Phe have different effects on the positioning of a transmembrane helix in the microsomal membrane, *Biochemistry* 38 (1999) 9778–9782.
- [8] J.A.A. Demmers, E. van Duijn, J. Haverkamp, D.V. Greathouse, R.E. Koeppe II, A.J.R. Heck, J.A. Greathouse, Interfacial positioning and stability of transmembrane peptides in lipid bilayers studies by combining hydrogen/deuterium exchange and mass spectroscopy, *J. Biol. Chem.* 276 (2001) 34501–34508.
- [9] P.C.A. van der Wel, E. Strandberg, J.A. Killian, R.E. Koeppe, Geometry and intrinsic tilt of a tryptophan-anchored transmembrane  $\alpha$ -helix determined by  $^2\text{H}$  NMR, *Biophys. J.* 83 (2002) 1479–1488.
- [10] T.M. Weiss, P.C.A. van der Wel, J.A. Killian, R.E. Koeppe II, H.W. Huang, Hydrophobic mismatch between helices and lipid bilayers, *Biophys. J.* 84 (2003) 379–385.
- [11] M.R.R. de Planque, E. Goormaghtigh, D.V. Greathouse, R.E. Koeppe II, J.A.W. Kruijtzter, R.M.M. Liskamp, B. de Kruijff, J.A. Killian, Sensitivity of single membrane-spanning  $\alpha$ -helical peptides to hydrophobic mismatch with a lipid bilayer: Effects on backbone structure, orientation and extent of membrane incorporation, *Biochemistry* 40 (2001) 5000–5010.
- [12] S. Sharpe, K.R. Barber, C.W.M. Grant, D. Goodyear, M.R. Morrow, Organisation of model helical peptides in lipid bilayers: insight into the behaviour of single-span protein transmembrane domains, *Biophys. J.* 83 (2002) 345–358.
- [13] W.M. Yau, W.C. Wimley, K. Gawrisch, S.H. White, The preference of tryptophan for membrane interfaces, *Biochemistry* 37 (1998) 14713–14718.
- [14] H.C. Gaede, W. Yau, K. Gawrisch, Electrostatic contributions to indole–lipid interactions, *J. Phys. Chem. B* 109 (2005) 13014–13023.
- [15] T. Hessa, H. Kim, K. Bihlmaier, C. Lundin, J. Boekel, H. Andersson, I. Nilsson, S.H. White, G. von Heijne, Recognition of transmembrane helices by the endoplasmic reticulum translocon, *Nature* 433 (2006) 377–381.
- [16] A. Senes, D.C. Chadi, P.B. Law, R.F.S. Walters, V. Nanda, W.F. DeGrado, Ez, a depth-dependent potential for assessing the energies of amino acid side-chains into membranes: Derivation and applications to determining the orientation of transmembrane and interfacial helices, *J. Mol. Biol.* 366 (2007) 436–448.
- [17] S. Tanizaki, M. Feig, A generalized born formalism for heterogeneous dielectric environments: Application to the implicit modeling of biological membranes, *J. Chem. Phys.* 122 (2005) 124706–124719.
- [18] S. Dorairaj, T.W. Allen, On the thermodynamic stability of a charged arginine side chain in a transmembrane helix, *Proc. Natl. Acad. Sci. U. S. A.* 104 (2007) 4943–4948.
- [19] D. Bemporad, J.W. Essex, C. Luttmann, Permeation of small molecules through a lipid bilayer: A computer simulation study, *J. Phys. Chem. B* 108 (2004) 4875–4884.
- [20] M.P. Aliste, D.P. Tieleman, Computer simulation of partitioning of ten pentapeptides ace-wlxll at the cyclohexane/water and phospholipid/water interfaces, *BMC Biochem.* 6 (2005) 30–31.
- [21] J.L. MacCallum, W.F.D. Bennett, D.P. Tieleman, Partitioning of amino acid side chains into lipid bilayers: Results from computer simulations and comparison to experiment, *J. Gen. Physiol.* 129 (2007) 371–377.
- [22] M. Ulmschneider, J. Ulmschneider, M. Sansom, A. Di Nola, A generalized born implicit membrane representation compared to experimental insertion free energies, *Biophys. J.* 92 (2007) 2338–2349.
- [23] W. Gu, S.J. Rahi, V. Helms, Solvation free energies and transfer free energies for amino acids from hydrophobic solution to water solution from a very simple residue model, *J. Phys. Chem. B* 108 (2004) 5806–5814.
- [24] E. Granseth, G. von Heijne, A. Elofsson, A study of the membrane–water interface region of membrane proteins, *J. Mol. Biol.* 346 (2005) 377–385.
- [25] S.H. White, W.C. Wimley, Hydrophobic interactions of peptides with membrane interfaces, *Biochim. Biophys. Acta* 1376 (1998) 339–352.
- [26] J.A. Killian, G. von Heijne, How proteins adapt to a membrane–water interface, *TIBS* 25 (2000) 429–434.
- [27] M. Monne, I. Nilsson, M. Johansson, N. Elmhed, G. von Heijne, Positively and negatively charged residues have different effects on the position in the membrane of a model transmembrane helix, *J. Mol. Biol.* 284 (1998) 1177–1183.
- [28] W. Ruan, V. Becker, U. Klingmüller, D. Langosch, The interface between the self-assembling erythropoietin receptor transmembrane segments corresponds to a heptad repeat pattern, *J. Biol. Chem.* 279 (2004) 3273–3279.
- [29] A. Grossfield, J. Sachs, T.B. Woolf, Dipole lattice membrane model for protein calculation, *Proteins* 41 (2000) 211–233.
- [30] F.N.R. Petersen, M. Jensen, C.H. Nielsen, Interfacial tryptophan residues: a role for the cation–p effect? *Biophys. J.* 89 (2005) 3985–3996.
- [31] K.E. Norman, H. Nymeyer, Indole localization in lipid membranes revealed by molecular simulation, *Biophys. J.* 91 (2006) 2046–2054.
- [32] A.C.V. Johansson, E. Lindahl, Position-resolved free energy of solvation for amino acids in lipid membranes from molecular dynamics simulations, *Proteins* 70 (2008) 1332–1344.
- [33] A.C.V. Johansson, E. Lindahl, Amino acid solvation structure in transmembrane helices from molecular dynamics simulations, *Biophys. J.* 91 (2006) 4450–4463.
- [34] M.A. Lomize, A.L. Lomize, I.D. Pogozheva, H.I. Mosberg, OPM: orientations of proteins in membranes database, *Bioinformatics* 22 (2006) 623–625.
- [35] D. Sengupta, L. Meinhold, D. Langosch, G.M. Ullmann, J.C. Smith, Understanding the energetics of helical-peptide orientation in membranes, *Proteins* 58 (2005) 913–922.
- [36] D. Sengupta, R.N. Behera, J.C. Smith, G.M. Ullmann, The  $\alpha$ -helix dipole: screened out? *Struct.* 13 (2005) 849–855.
- [37] A. R. Leach (Ed.), *Molecular Modelling: Principles and applications*, Pearson Education Limited, 2001.
- [38] H.A. Stern, S.E. Feller, Calculation of dielectric permittivity profile for a nonuniform system: application to a lipid bilayer simulation, *J. Chem. Phys.* 118 (2003) 3401–3411.
- [39] H.G.L. Coster, J.R. Smith, The molecular organization of bimolecular lipid membranes. a study of low frequency Maxwell–Wagner impedance dispersion, *Biochim. Biophys. Acta* 373 (1974) 151–164.
- [40] F. Zhou, K. Schulten, Molecular dynamics study of a membrane–water interface, *J. Phys. Chem.* 99 (1995) 2194–2207.
- [41] R. Cseh, R. Benz, Interaction of phloretin with lipid monolayers: Relationship between structural changes and dipole potential change, *Biophys. J.* 77 (1999) 1477–1488.
- [42] G. Cevc, A. Watts, D. Marsh, Titration of the phase transition of phosphatidylserine bilayer membranes. effects of pH, surface electrostatics, ion binding and head group hydration, *Biochemistry* 20 (1981) 4955–4965.
- [43] P.I. Lelkes, I.R. Miller, Perturbations of membrane structure by optical probes: location and structural sensitivity of merocyanine 540 bound to phospholipid membranes, *J. Mol. Biol.* 52 (1980) 1–15.
- [44] W. Im, D. Beglov, B. Roux, Continuum solvation model: computation of electrostatic forces from numerical solutions to the Poisson–Boltzmann equation, *Comp. Phys. Commun.* 109 (1998) 1–17.
- [45] B.R. Brooks, R.E. Bruccoleri, B.D. Olafson, D.J. States, S. Swaminathan, M. Karplus, CHARMM: A program for macromolecular energy, minimization, and dynamics calculation, *J. Comp. Chem.* 4 (1983) 187–217.
- [46] M. Nina, D. Beglov, B. Roux, Atomic Born radii for continuum electrostatic calculations based on molecular dynamics, *J. Phys. Chem.* 101 (1997) 5239–5248.
- [47] Y. Nozaki, C. Tanford, The solubility of amino acids and two glycine peptides in aqueous ethanol and dioxane solutions. establishment of a hydrophobicity scale, *J. Biol. Chem.* 246 (1971) 2211–2217.
- [48] D. Sitkoff, N. Ben-Tal, B. Honig, Calculation of alkane to water solvation free energies using continuum solvent models, *J. Phys. Chem.* 100 (1996) 2744–2752.
- [49] A. Kessel, D.S. Cafiso, N. Ben-Tal, Continuum solvent model calculations of alamethicin–membrane interactions: thermodynamic aspects, *Biophys. J.* 78 (2000) 571–583.
- [50] D. Murray, L. Hermida-Matsumoto, C.A. Buser, J. Tsang, C.T. Sigal, N. Ben-Tal, Electrostatics and the membrane association of Src: theory and experiment, *Biochemistry* 37 (1998) 2145–2159.
- [51] N. Ben-Tal, A. Ben-Shaul, A. Nicholls, B. Honig, Free-energy determinants of  $\alpha$ -helix insertion into bilayers, *Biophys. J.* 70 (1996) 1803–1812.
- [52] A.D. Petelska, Z.A. Figaszewski, Effect of pH on the interfacial tension of lipid bilayer membrane, *Biophys. J.* 78 (2000) 812–817.
- [53] B. Lee, F.M. Richards, The interpretation of protein structures: estimation of static accessibility, *J. Mol. Biol.* 55 (1971) 379–400.
- [54] E. Strandberg, J. Killian, Snorkeling of lysine side chains in transmembrane helices: how easy can it get? *FEBS Letters* 544 (2003) 69–73.
- [55] T. Nyholm, S. Ozdircakan, J. Killian, How protein transmembrane segments sense the lipid environment, *Biochemistry* 46 (2007) 1457–1465.
- [56] D. Eisenberg, R.M. Weiss, T.C. Terwilliger, The helical hydrophobic moment: a measure of the amphiphilicity of a helix, *Nature* 299 (1982) 371–374.
- [57] T. Simonson, A.T. Bringer, Solvation free energies estimated from macroscopic continuum theory: An accuracy assessment, *J. Phys. Chem.* 98 (1994) 4683–4694.
- [58] A. Radzicka, R. Wolfenden, Comparing the polarities of the amino acids: Side-chain distribution coefficients between the vapor phase, cyclohexane, 1-Octanol, and neutral aqueous solution, *Biochemistry* 27 (1988) 1664–1670.
- [59] W. Wimley, T. Creamer, S. White, Solvation energies of amino acid side chains and backbone in a family of host-guest pentapeptides, *Biochemistry* 35 (16) (1996) 5109–5124.
- [60] B. Roux, Lonely arginine seeks friendly environment, *J. Gen. Physiol.* 130 (2007) 233–236.
- [61] T.W. Allen, Modeling charged protein side chains in lipid membranes, *J. Gen. Physiol.* 130 (2007) 237–240.